PHYSICAL REVIEW C
NUCLEAR PHYSICS

THIRD SERIES, VOLUME 28, NUMBER 3 SEPTEMBER 1983

^{14}N($\vec{p}$,p')^{14}N(2.31 MeV) reaction at 159.4 MeV

T. N. Taddeucci and J. Rapaport
Department of Physics, Ohio University, Athens, Ohio 45701

C. C. Foster
Indiana University Cyclotron Facility, Bloomington, Indiana 47405

J. R. Comfort*
Department of Physics and Astronomy, University of Pittsburgh, Pittsburgh, Pennsylvania 15260 and Physics Department, Arizona State University, Tempe, Arizona 85287
(Received 25 February 1983)

Differential cross-section and analyzing-power angular distributions have been measured for the elastic scattering of 159.4 MeV protons on ^{14}N and for the inelastic transitions to the 2.31-MeV and 3.95-MeV states. Elastic-scattering data for $\vec{p}+{}^{12}$C and inelastic data for the ^{12}C($\vec{p}$, p')^{12}C(4.44 MeV) reaction have also been obtained at the same energy as a normalization check. The ^{14}N($\vec{p}$,p')^{14}N(2.31 MeV) transition has been analyzed in the distorted-wave impulse approximation. This transition has long been regarded as a favorable test for the tensor component of the effective nucleon-nucleon interaction. Calculations employing wave functions that provide the necessary cancellation of the $L=0$ central-interaction transition strength do not provide a good description of the differential cross-section angular distribution. It is suggested that more complicated reaction mechanisms, e.g., (p,d)(d,p') contributions, may be needed to describe this transition.

[NUCLEAR REACTIONS ^{12}C($\vec{p}$,p), ($\vec{p}$,p'), $E_x=4.44$ MeV; ^{14}N($\vec{p}$,p), ($\vec{p}$,p'), $E_x=2.31$, 3.95 MeV; $E_p=159.4$ MeV. Measured $\sigma(\theta)$, $A_y(\theta)$, $\theta_{lab}=7.5°-45°$. DWIA analysis of 2.31-MeV transition.]

I. INTRODUCTION

We report here measurements of the differential cross sections and analyzing powers for proton elastic scattering on ^{12}C and ^{14}N and for the inelastic reactions ^{14}N($\vec{p}$,p')^{14}N(2.31 MeV), ^{14}N($\vec{p}$,p')^{14}N(3.95 MeV), and ^{12}C($\vec{p}$,p')^{12}C(4.44 MeV) at $E_p=159.4$ MeV. The differential cross-section data are qualitatively similar to those previously obtained[1] at $E_p=122$ MeV; however, the results presented here represent the first measurements of the analyzing powers for inelastic scattering of protons by ^{14}N at intermediate energies.

The ^{14}N(p,p')^{14}N(2.31 MeV) reaction is related to the highly retarded ^{14}C(β^-)^{14}N(g.s.) decay in the sense that it connects the ^{14}N ground state to the isobaric analog of the ^{14}C ground state. The approximate proportionality between the β-decay matrix element and the $L=0$ central-interaction (p,p') transition amplitude thus results in the suppression of this normally dominant amplitude. Because of this suppression, the ^{14}N(p,p')^{14}N(2.31 MeV) reaction has long been recognized as a potentially sensitive test for the strength of the effective tensor interaction in inelastic proton scattering.[2]

Previous analyses of this reaction in the distorted-wave Born approximation (DWBA) and the distorted-wave impulse approximation (DWIA) over the energy range $E_p=24.8-122$ MeV have been largely unsuccessful in reproducing all but the most qualitative features of the differential cross-section angular distributions.[1-3] On the basis of comparison with differential cross sections alone, it has been difficult to single out the source of the disagreement between theory and experiment. Measurements of spin-dependent observables, which would provide additional constraints for the theoretical parameters, have been scarce. Cornelius, Moss, and Yamaya have measured the spin-flip probability at two angles at $E_p=32$ MeV.[4] Their data seem to indicate a strong contribution from the tensor part of the effective interaction, but this result is not conclusive because the DWBA reproduces only the qualitative trend of their data and not the magnitudes.

 ©1983 The American Physical Society

Recently, Aoki *et al.* have measured differential cross section and analyzing power angular distributions at $E_p = 21$ MeV.[5] Their DWBA analysis includes contributions from (p,d)(d,p′) intermediate channels and gives somewhat better fits to the data than single-step calculations.

In our analysis of the present data, discussed in Sec. III, we restrict ourselves to the single-step DWIA. The need for two-step contributions to the transition amplitude will be discussed only as a possible remedy for difficulties encountered by the standard DWIA.

II. EXPERIMENTAL TECHNIQUE

Targets of ^{14}N and ^{12}C were bombarded with 159.4-MeV polarized protons from the Indiana University Cyclotron Facility (IUCF). The ^{14}N target consisted of 12.3 mg/cm^2 of melamine ($C_3H_6N_6$) evaporated onto a 100-μg/cm^2 carbon backing. The ^{12}C target was of natural graphite with a thickness of 6.14 mg/cm^2 and was used for normalization purposes.

Beam polarization was periodically monitored with a p+^{4}He polarimeter located in the beam line between the injector and main-stage cyclotrons. The beam was automatically cycled between spin-up and spin-down orientations at 60-sec intervals during both data taking and polarization measurements. During the course of the experiment the polarization for the two spin orientations did not vary by more than ± 0.02 from average values of $P\uparrow = 0.70$ and $P\downarrow = -0.72$. For any given run the estimated uncertainty in the polarization for either spin orientation is less than $|\delta P/P| = 0.01$.

Reaction-product particles scattered into the correct angle were momentum analyzed in the IUCF quadrupole-dipole-dipole-quadrupole spectrograph operating in a dispersion-matched mode and were detected in a helical-cathode position-sensitive proportional chamber.[6] Particle identification was accomplished with a fast plastic-scintillator ΔE-E telescope following the proportional chamber. Software-defined proton events were sorted online and stored as 1-d arrays on magnetic tape. Dead time was measured by feeding pulser signals triggered by the current integrator through the entire electronics system. Event rates were typically below about 1 kHz with corresponding dead times of 14% or less.

Due to the weakness of the 2.31-MeV transition in ^{14}N it was not practical at forward angles to have both elastically-scattered and inelastically-scattered protons on the focal plane at the same time. A thick lead block placed in front of the focal plane at the position of the elastic proton group removed this intense peak without increasing the background.

Simple summing techniques have been used to extract yields for the peaks corresponding to ^{12}C and ^{14}N elastic scattering and for the ^{12}C(4.44 MeV), ^{14}N(2.31 MeV), and ^{14}N(3.95 MeV) excited states. All five proton energy groups are visible in spectra obtained with the melamine target due to its 30.3% ^{12}C content. A spectrum obtained with the spin-up beam at a laboratory angle of 27.5° is shown in Fig. 1. Comparison of the ^{12}C yields obtained from this target with those obtained from the graphite target served as a relative normalization check. At forward angles the ^{12}C(4.44 MeV) peak was well separated from underlying ^{14}N states, while at larger angles the ^{12}C elastic peak was well resolved from the ^{14}N elastic peak. Absolute ^{12}C differential cross sections obtained by use of the melamine and the graphite nominal target thicknesses agree to better than 5%. We thus conclude that the relative normalization of the ^{14}N and ^{12}C cross sections reported here is accurate to better than 5%. Individual uncertainties in target thickness (5%), charge collection (2%), and background subtraction (usually less than 3%, but 10% for the weak 2.31-MeV transition) yield a combined uncertainty of about 6% for the absolute normalization of the cross sections.

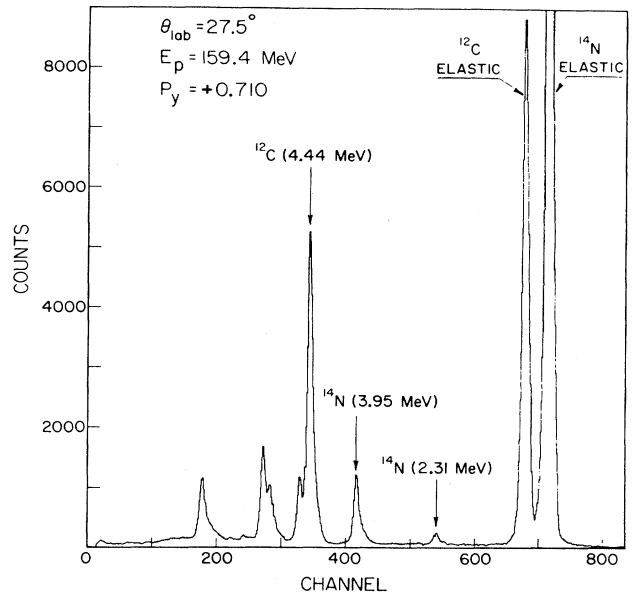

FIG. 1. Spin-up ($\vec{p}$,p′) spectrum obtained with a melamine ($C_3H_6N_6$) target. The unidentified peaks correspond to states in ^{14}N.

III. MICROSCOPIC DWIA ANALYSIS

In this section we describe the results of microscopic DWIA calculations and their comparison to the experimental angular distributions. The motivation and philosophy behind specific aspects of the calculations have been extensively discussed elsewhere.[1,7] The calculations have been carried out with a modified version of the code DWBA70,[8] which computes both direct and knockout exchange amplitudes exactly. In the next three subsections we briefly summarize those details pertinent to the present analysis.

A. Optical potential

The elastic-scattering differential cross-section and analyzing-power angular distributions are shown in Figs. 2 and 3. The differential cross sections are displayed in ratio to the Rutherford cross section

$$\sigma_R(\theta) = Z^2 e^2 E^2 / [4k^4 \sin^4(\theta/2)] ,$$

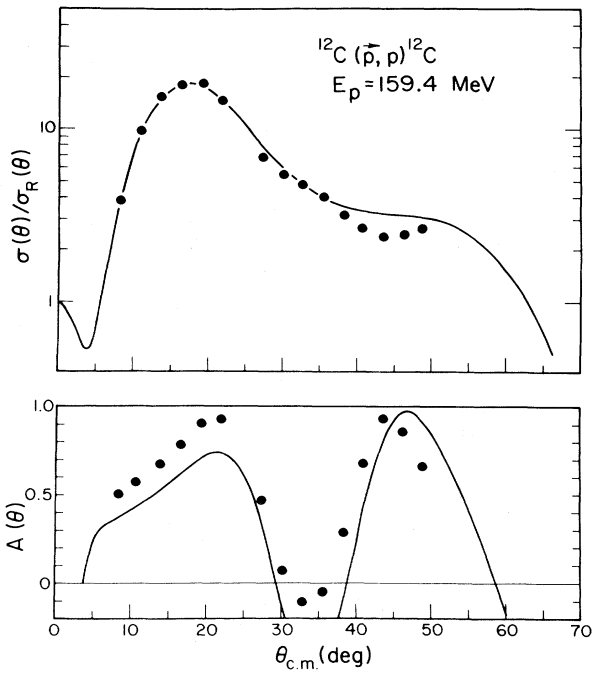

FIG. 2. Differential cross sections and analyzing powers for elastic scattering of 159.4-MeV protons on ^{12}C. The differential cross sections are plotted in ratio to the Rutherford cross sections.

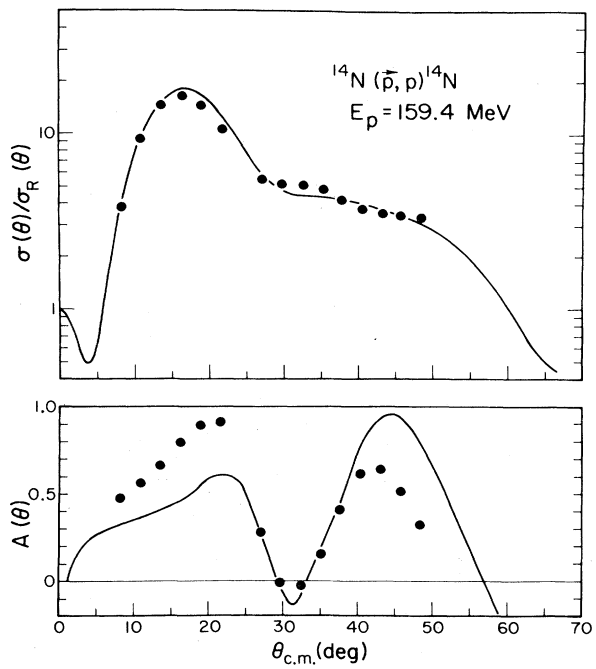

FIG. 3. Differential cross sections and analyzing powers for elastic scattering of 159.4-MeV protons on ^{14}N. The differential cross sections are plotted in ratio to the Rutherford cross sections.

where k and E are the relativistic momentum and reduced energy, and $\hbar=c=1$. The solid lines in these figures represent the results of independent parameter searches made with the optical-model search code CUPID.[9] The optical parameters determined by these fits are presented in Table I. The DWIA calculations described in the following sections employed the ^{14}N parameters in this table. Despite the differences between the ^{12}C and ^{14}N parameters, test calculations show that the DWIA results for the inelastic transitions are insensitive to the specific choice of parameter set.

B. Effective interaction

The effective interaction between the ith target nucleon and the projectile may be represented as

$$V_{\text{eff}}(r)=V_0(r)+V_\sigma(r)\vec{\sigma}_i\cdot\vec{\sigma}_p+V_\tau(r)\vec{\tau}_i\cdot\vec{\tau}_p+V_{\sigma\tau}(r)\vec{\sigma}_i\cdot\vec{\sigma}_p\vec{\tau}_i\cdot\vec{\tau}_p$$

$$+[V_{LS}(r)+V_{LS\tau}(r)\vec{\tau}_i\cdot\vec{\tau}_p]L\cdot S+[V_T(r)+V_{T\tau}(r)\vec{\tau}_i\cdot\vec{\tau}_p]S_{ip}\ , \qquad (1)$$

TABLE I. The optical potentials determined from fits to p+^{12}C and p+^{14}N elastic scattering at $E_p=159.4$ MeV. The potentials are defined by $U(r)=V_C(r)+Vf_R(r)+iWf_I(r)+V_{so}(r)(1/r)(d/dr)f_{so}(r)\vec{l}\cdot\vec{s}$, where V_C is the Coulomb potential for a uniformly charged sphere, $f_i(r)=[1+\exp(x_i)]^{-1}$, and $x_i=(r-R_i)/a_i$ with $R_i=r_iA^{1/3}$. Well depths have units MeV and lengths have units fm. The potentials are defined for use with relativistic kinematics.[a] Also listed are the χ^2 per point for the cross section and analyzing power fits.

Target	V	r_R	a_R	W	r_I	a_I	V_{so}	r_{so}	a_{so}	r_C	χ^2_σ/N	χ^2_A/N
^{12}C	−13.9	1.20	0.67	−13.3	1.24	0.62	18.5	0.90	0.50	1.20	4.93	95.7
^{14}N	−18.0	1.20	0.62	−13.2	1.24	0.60	18.8	0.90	0.50	1.20	30.5	247

[a]Reference 20.

where

$$S_{ip}=3(\vec{\sigma}_i\cdot\hat{r})(\vec{\sigma}_p\cdot\hat{r})-\vec{\sigma}_i\cdot\vec{\sigma}_p$$

is the tensor operator. The strengths and radial dependence of the various interaction terms are functions of the bombarding energy. At low energies, $E_p \leq 100$ MeV, it is necessary to resort to theoretically-developed G-matrix interactions (e.g., see Ref. 10) or to simple phenomenological interactions that have been calibrated against transitions for which the optical potential, reaction mechanism, and nuclear wave functions are well established.[11] Indeed, as was mentioned in the Introduction, the ^{14}N(p,p′)^{14}N (2.31 MeV) transition has been considered a good candidate for calibration of the tensor interaction. At higher energies, $E_p \geq 100$ MeV, the usual strategy has been to use a t-matrix interaction that is derived directly from the free nucleon-nucleon interaction, and thus has no free parameters to calibrate.[12] This procedure, with the interaction strengths determined solely by the free N-N amplitudes, is the essence of the impulse approximation (DWIA). In this work we employ the 140-MeV t-matrix interaction of Love and Franey (LF).[13] This interaction consists of sums of Yukawa (e^{-x}/x, $x=r/a$) radial shapes with varying strengths for the central and spin-orbit components and $r^2\times$Yukawa forms for the tensor interaction. The interaction strengths have both real and imaginary terms.

C. Wave functions

Harmonic-oscillator single-particle wave functions have been used to describe the bound target nucleons. The oscillator parameters are taken from Ref. 1, but have been corrected for center-of-mass motion,[7] i.e., for the g.s.→2.31-MeV transition

$$\mu=0.588(14/13)^{1/2}\ \mathrm{fm}^{-1}$$

and for the g.s.→3.95-MeV transition

$$\mu=0.595(14/13)^{1/2}\ \mathrm{fm}^{-1}\ .$$

The calculations are in general insensitive to small variations in these parameters. We have used four sets of shell-model wave functions in the analysis of the 2.31-MeV transition: wave functions derived from the Cohen-Kurath (CK) "POT" and "(8–16)2BME" two-body matrix elements,[14] wave functions derived by Ensslin *et al.* from electron scattering and other experimental data,[15] and wave functions constructed by Visscher and Ferrell (VF).[16] These wave functions are input into the code DWBA70 in the form of spectroscopic coefficients defined by

$$Z_J(j_p j_h)=(\hat{J}_i\hat{J})^{-1}\langle f||(a^\dagger_{j_p}\otimes b^\dagger_{j_h})^{JT}_{T_z}||i\rangle\ , \tag{2}$$

where the particle-hole operator $a^\dagger b^\dagger$ is coupled to spin transfer J and isospin transfer (T,T_z), and $\hat{J}\equiv(2J+1)^{1/2}$. For purposes of comparison, it is desirable to express the spectroscopic coefficients in a representation where the transferred quanta (JLS) are explicit[17]:

$$Z_J(LS)=\sum_{j_p j_h}\hat{j}_p\hat{j}_h\hat{L}\,\hat{S}\begin{Bmatrix} l_p & \frac{1}{2} & j_p \\ l_h & \frac{1}{2} & j_h \\ L & S & J \end{Bmatrix}Z_J(j_p j_h)\ . \tag{3}$$

The selection rules for the direct amplitude for $1^+\rightarrow 0^+$ transitions require that $(JLS)=(101)$ or (121). The spectroscopic coefficients $Z_1(01)$ and $Z_1(21)$ thus control the relative amounts of $L=0$ and $L=2$ strength in the direct (p,p′) amplitude. The remaining two coefficients, $Z_1(11)$ and $Z_1(10)$, affect only the knockon exchange amplitudes.[7,18] The spectroscopic coefficients for the ^{14}N(p,p′)^{14}N(2.31 MeV) transition are listed in Table II in both the $Z_J(j_p j_h)$ and $Z_J(LS)$ representations.

D. The 2.31-MeV state in ^{14}N

The experimental differential cross-section and analyzing-power angular distributions for the ^{14}N($\vec{p}$,p′)^{14}N(2.31 MeV) transition are shown in Figs.

TABLE II. Spectroscopic coefficients for the ^{14}N(p,p′)^{14}N(2.31 MeV) transition. The coefficients are given in the $Z_J(j_p j_h)$ representation (upper half) and in the $Z_J(LS)$ representation (lower half).

Wave function	$Z_1(1/2,1/2)$	$Z_1(3/2,3/2)$	$Z_1(1/2,3/2)$	$Z_1(3/2,1/2)$
CK POT[a]	−0.515	0.0126	−0.0241	0.0770
CK 2BME[b]	−0.506	0.0042	−0.0347	0.118
Ensslin[c]	−0.297	−0.0144	0.138	0.228
VF[d]	−0.518	−0.0122	−0.0262	0.143
	$Z_1(01)$	$Z_1(21)$	$Z_1(11)$	$Z_1(10)$
CK POT[a]	0.0517	−0.477	0.0374	−0.200
CK 2BME[b]	0.0169	−0.483	0.0588	−0.185
Ensslin[c]	0.0	−0.279	0.259	−0.121
VF[d]	0.0	−0.494	0.0585	−0.197

[a]Cohen-Kurath, Ref. 14.
[b]Cohen-Kurath, Ref. 14, (8–16)2BME.
[c]Reference 15.
[d]Visscher-Ferrell, Ref. 16.

4–7. The DWIA results displayed in these figures clearly show the effect of increasing the $L=0$ contribution to the transition amplitude. The curves in Fig. 4 correspond to DWIA calculations employing the Ensslin wave functions, for which the $L=0$ central-interaction amplitude is zero. The solid lines in this figure are the results of calculations employing the full LF 140-MeV interaction, while the dashed lines correspond to a calculation with the central interaction only. The analyzing power angular distribution is reproduced best by the central interaction calculation, but this gives the poorest description of the differential cross sections.

The wave functions of Visscher and Ferrell[16] were also constructed to reproduce the $L=0$ central-interaction cancellation, and are probably more realistic than those of Ensslin.[15,19] The Ensslin wave functions describe the ^{14}C ground state as almost entirely $|\,^1P_0\rangle$, while in the VF wave functions (and in the two CK wave functions as well) the dominant component is $|\,^1S_0\rangle$. Despite these differences, the calculated cross-section angular distributions for the Ensslin and VF wave functions are very similar in shape (Fig. 5). The differential cross sections obtained by using the VF wave functions are larger than those obtained from the Ensslin wave functions because of the larger $L=2$ amplitude [$Z_1(21)$; see Table II], while the analyzing power angular distributions differ primarily because of the large abnormal-parity $Z_1(11)$ amplitude associated with the Ensslin wave functions. When this amplitude is removed, the resulting analyzing-power distribution looks very similar to that obtained with the VF wave functions.

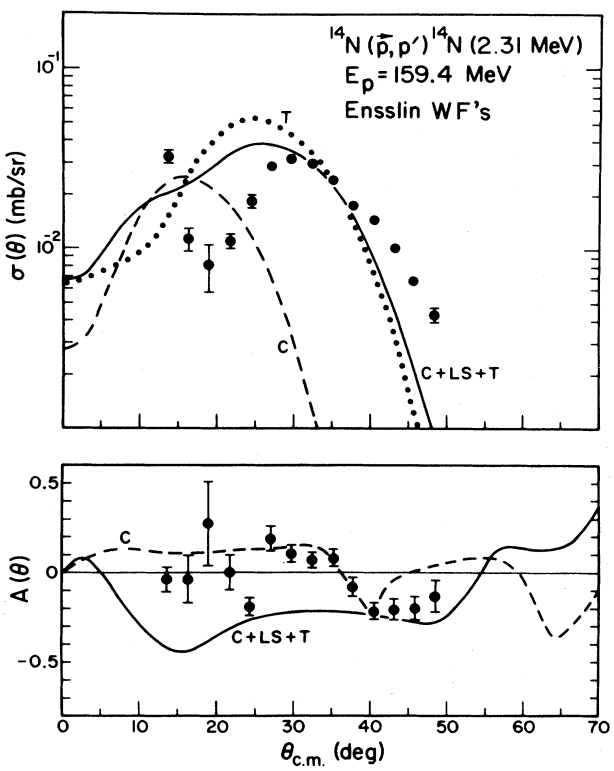

FIG. 4. Differential cross sections and analyzing powers for the ^{14}N(p,p')^{14}N(2.31 MeV) reaction at $E_p=159.4$ MeV. Error bars represent counting statistics only. The wave functions of Ensslin *et al.* (Ref. 15) were used in the DWIA calculations. The solid line is the result of a calculation with the full LF 140-MeV *t*-matrix interaction (Ref. 13): central (C)+spin-orbit(LS) + tensor(T). The dashed line is the result of a calculation employing the central interaction only, while the dotted line results from a calculation with the tensor interaction only.

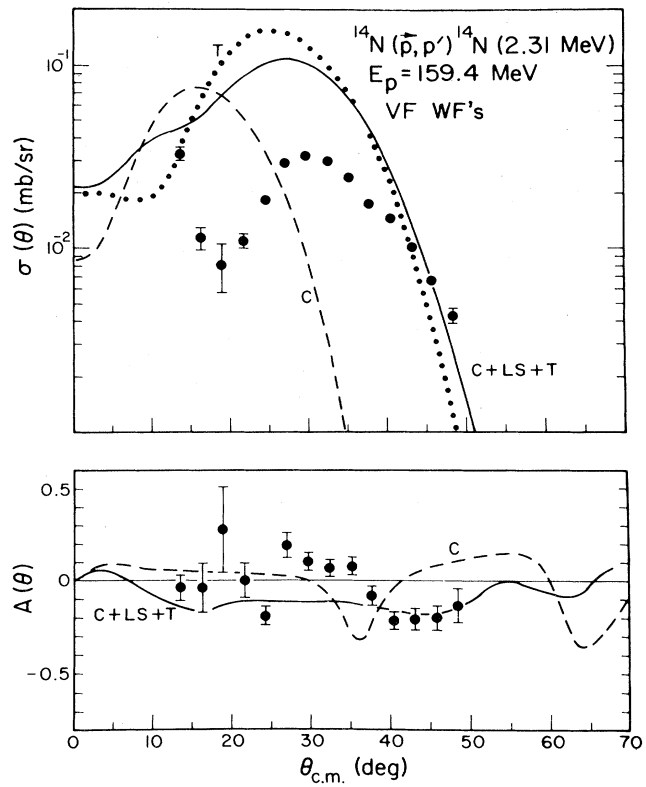

FIG. 5. The results of DWIA calculations employing the wave functions of Visscher and Ferrell (Ref. 16). See also the caption of Fig. 4.

In Fig. 6 are shown the results of calculations employing the CK 2BME wave functions. These wave functions result in more $L=0$ strength than required by β decay, but give better qualitative fits to the shapes of the differential cross section and analyzing power angular distributions. Our criterion for "goodness of fit" for the differential cross sections is the simultaneous reproduction of the forward-angle maximum and the minimum at $\theta=20°$. These two features are persistent characteristics of the angular distribution for this reaction for $25<E_p<120$ MeV.[1–3] (The forward-angle maximum is not as evident in the present results because of the limited data in this region.) Examination of the calculations indicates that the experimental differential cross-section pattern of maximum-minimum-maximum is produced by alternate constructive-destructive interference between the central and tensor amplitudes.

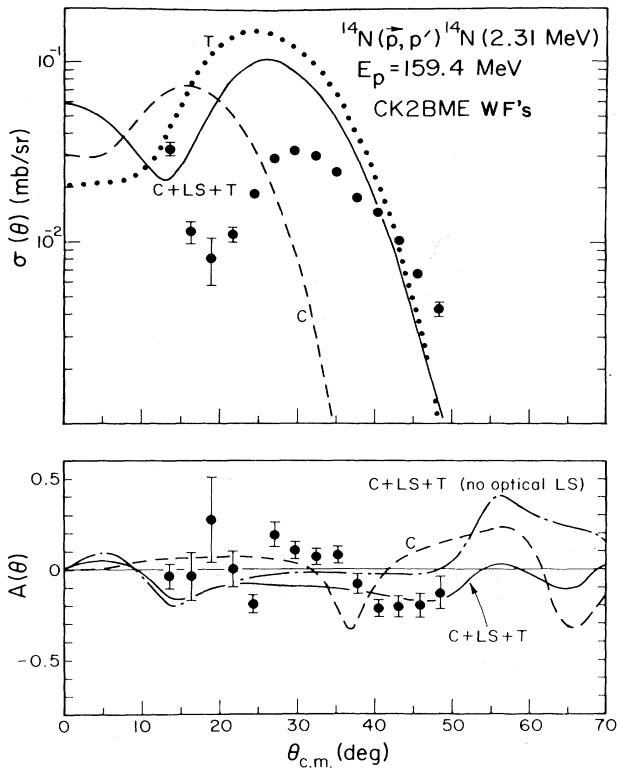

FIG. 6. The results of DWIA calculations with the Cohen-Kurath "(8–16)2BME" wave functions (Ref. 14). The dotted-dashed line is the analyzing power distribution in the plane-wave approximation. See also the caption of Fig. 4.

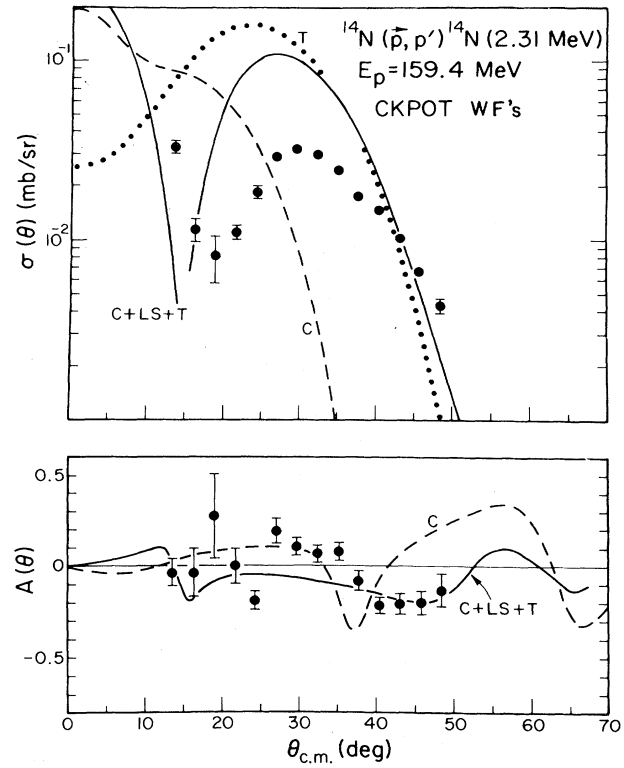

FIG. 7. The results of DWIA calculations with the Cohen-Kurath "(8–16)POT" wave functions (Refs. 14 and 17). See also the caption of Fig. 4.

The results of calculations employing the CK POT wave functions are shown in Fig. 7. These wave functions contribute about nine times more central $L=0$ strength than the CK 2BME wave functions. Here, the interference between the central and tensor amplitudes is particularly dramatic. Despite the large difference in the differential cross-section angular distributions, the analyzing-power angular distributions for the two Cohen-Kurath wave function sets are very similar. This similarity is not a consequence of the predominance of distortion effects. A plane-wave calculation, plotted as the dotted-dashed line in Fig. 6, shows that the basic shape of the analyzing power distribution for this transition is determined by the microscopic form factor.

The results discussed above show that qualitative reproduction of the shape of the differential cross section angular distribution requires more central $L=0$ transition strength than is indicated by the analogous β decay. If we accept the β-decay comparison as a valid criterion for wave function selection, then the problems encountered in trying to reproduce the differential cross section angular distribution are due to either the effective interaction or the assumed reaction mechanism.

Auxiliary calculations employing different interactions give results that are both qualitatively and quantitatively (within 10%) similar to those shown in Figs. 4–7. The interactions tested were the LF 210-MeV t-matrix interaction[13] and the Love 140-MeV t-matrix interaction.[12]. In addition, an alternative tensor interaction derived from fits to the Sussex oscillator matrix elements[12] was substituted for the "standard" tensor terms in the above interactions. The differential cross sections are changed very little by this alternative tensor interaction while the analyzing-power angular distributions (for the CK wave functions) become small ($|A_y|<0.05$) for $\theta<25°$ and more negative ($A_y<-0.2$) for $\theta>45°$. Finally, the effects of the tensor exchange amplitudes may be tested by removing the $Z_1(11)$ component (Table II) from the wave functions. The tensor exchange contributions are driven mainly by this abnormal-parity amplitude.[7,18] The differential cross sections obtained from calculations with this term removed show little difference from the results presented in Figs. 4–7, even for the Ensslin wave functions, for which $Z_1(11)$ is relatively large.

The above tests of the sensitivity of the calculation to details of the interaction are not exhaustive, but they suggest that only gross modifications of the interaction are likely to produce better fits to the cross section and analyzing power angular distributions. Such modifications do not seem warranted, however, since the interactions tested have produced generally satisfactory results when applied to other transitions.[1,7,18]

The failure of the standard single-step DWIA, employing reasonable optical parameters, wave functions, and in-

teractions, strongly suggests the need for consideration of more complex reaction mechanisms for this transition. Aoki *et al.*[5] have performed DWBA calculations including (p,d)(d,p') amplitudes in an analysis of this reaction at $E_p=21$ MeV. Inclusion of these two-step amplitudes produces a somewhat better fit to the differential cross sections at this energy and significantly improves the shape of the calculated analyzing-power distributions. These authors extended their two-step analysis to a maximum energy of $E_p=40$ MeV and compared the results to the data of Fox and Austin.[3] At 40 MeV the two-step amplitudes do not greatly change the shape of the differential cross section distribution. The main effect is an increase in magnitude due to constructive interference between the one-step and two-step contributions.

It has been argued that at intermediate energies ($E_p>100$ MeV) the effect of two-step contributions is largely accounted for when using optical potentials that accurately reproduce elastic scattering.[1,20] For weak transitions such as ^{14}N(p,p')^{14}N(2.31 MeV), however, it may be necessary to treat such effects explicitly. It is interesting to note that at 160 MeV the elastic two-step (p,d)(d,p) and presumably also the inelastic (p,d)(d,p') cross sections should be strongly forward peaked.[20] We have shown that wave functions that contribute too much $L=0$ strength give the best qualitative fits to the cross section angular distribution. It is possible that the improved shape obtained by adding more $L=0$ strength than is required by β decay is a consequence of mocking up in a crude way the presence of constructively interfering forward-peaked two-step amplitudes. Clearly, it should be interesting to explore this with more detailed calculations.

E. The 3.95-MeV state in ^{14}N and the 4.44-MeV state in ^{12}C

The differential cross-section and analyzing-power angular distributions for the ^{14}N($\vec{p}$,p')^{14}N(3.95 MeV) and ^{12}C($\vec{p}$,p')^{12}C(4.44 MeV) reactions are shown in Fig. 8. The $0^+\rightarrow 2^+$ isoscalar transition in ^{12}C involves angular momentum transfer of $J=2$ only, while the $1^+\rightarrow 1^+$ isoscalar transition in ^{14}N allows $J=0,1,2$. The $M1$ component ($J=1$) of the 3.95-MeV transition is very weak,[15] however, with the result that this transition is primarily $J=2$. Calculations performed with the CK 2BME wave functions and the LF 140-MeV t-matrix interaction indicate that the $J=2$ partial cross section for the 3.95-MeV transition contributes 95% of the total strength at the peak of the angular distribution ($\theta\simeq 20°$) in Fig. 8.

The similarity between the measured differential cross-section and analyzing-power angular distributions for these transitions is quite striking. The difference in magnitude between the differential cross sections is a reflection of the differing $E2$ transition strengths. The 3.95-MeV transition has a measured $E2$ strength[1,15,21,22] of

$$B(E2)\uparrow=3.3\pm0.2\ e^2\,\mathrm{fm}^4\ ,$$

while the $E2$ strength for the 4.44-MeV transition in ^{12}C is[23]

$$B(E2)\uparrow=38.8\pm2.5\ e^2\,\mathrm{fm}^4\ .$$

The ratio of these two transition strengths is 11.8 ± 1.0, in good agreement with the peak cross section ($\theta\simeq 20°$) ratio of 11.3 ± 0.6 for the analogous (p,p') transitions. This proportionality between $B(E2)$ and $\sigma(\theta)$ indicates that the

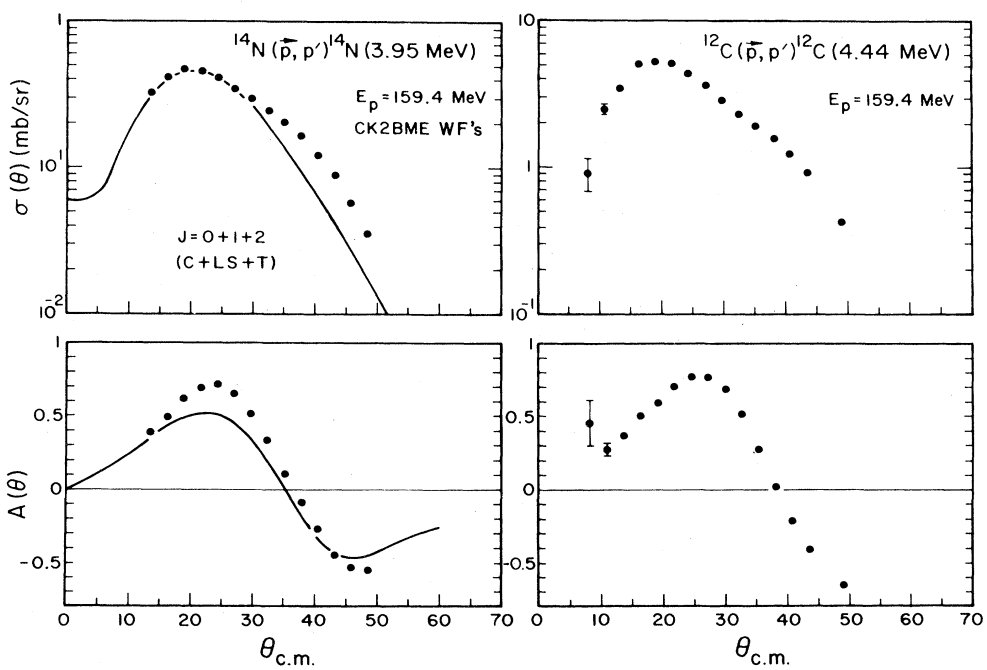

FIG. 8. Differential cross section and analyzing power angular distributions for the ^{14}N($\vec{p}$,p')^{14}N(3.95 MeV) transition (left) and the ^{12}C($\vec{p}$,p')^{12}C(4.44 MeV) transition (right). Error bars represent counting statistics only. The solid line is the result of a DWIA calculation employing the Cohen-Kurath (8—16)2BME wave functions and the LF 140-MeV t-matrix interaction. Contributions from all possible angular momentum transfers ($J=0,1,2$) are included.

calculated differential cross section angular distribution for the 3.95-MeV transition, shown as the solid line in Fig. 8, needs to be normalized upward by a factor of about 2. This calculation employed the CK 2BME wave functions, for which

$$B(E2)\uparrow = 1.7\ e^2\,\mathrm{fm}^4 .$$

The apparent good fit to the data is thus somewhat fortuitous. In Ref. 1, however, it is shown that a reasonable fit to the data may be restored by using an effective interaction with a different tensor component and a smaller imaginary central component.

For normal-parity isoscalar transitions, Kelly[24] has shown that density-dependent modifications to the effective interaction can lead to significant improvements in the calculated angular distributions. The high-q differential cross section enhancement that is one characteristic of such modifications might thus explain the discrepancy in shape between the experimental and DWIA angular distributions that is evident in Fig. 8 for $\theta > 30°$. It is also worth noting that the density dependent effects are much less important for isovector spin-dependent interactions[25] and should therefore have little effect on the transition to the 2.31-MeV state.

IV. SUMMARY AND CONCLUSIONS

Differential cross sections and analyzing powers have been measured for the ^{14}N($\vec{p}$,p′)^{14}N(2.31 MeV) reaction at $E_p = 159.4$ MeV. The differential cross section angular distribution for this transition has proven difficult to fit with standard single-step DWBA and DWIA calculations. It was hoped that the additional information and constraints provided by the analyzing power data would provide some clue to the nature of the theoretical difficulties. A DWIA analysis of this reaction has been carried out employing an optical potential obtained from fits to p+^{14}N elastic scattering data, a realistic t-matrix interaction obtained from fits to free N-N data, and wave functions chosen to reproduce to varying degrees the required inhibition of the $L=0$ central-interaction transition strength. The shape of the differential cross section angular distribution is best reproduced when using wave functions that allow too much $L=0$ strength (relative to the analogous β decay). The analyzing power comparisons are somewhat inconclusive. The best reproduction of the analyzing powers is obtained with wave functions that give small abnormal-parity $(JLS)=(111)$ amplitudes.

The results of the present analysis show that some mechanism is required for adding more $L=0$ strength to this transition than is required by comparison to β decay. Aoki *et al.*[5] have recently analyzed this transition at $E_p = 21$ MeV with two-step (p,d)(d,p′) amplitudes included in their calculations. Their work suggests that the constructively interfering and forward-peaked (at intermediate energies) (p,d)(d,p′) process may be a good candidate for improving the calculated differential cross section and analyzing power angular distributions. This effect is clearly worth further investigation.

ACKNOWLEDGMENTS

This work was supported in part by the National Science Foundation. Two of the authors (T.N.T. and J.R.C.) gratefully acknowledge the hospitality extended to them during lengthy visits at IUCF.

---

*Present address: Physics Department, Arizona State University, Tempe, AZ 85287.

[1]J. R. Comfort, Sam M. Austin, P. T. Debevec, G. L. Moake, R. W. Finlay, and W. G. Love, Phys. Rev. C 21, 2147 (1980).
[2]G. M. Crawley, S. M. Austin, W. Benenson, V. A. Madsen, F. A. Schmittroth, and M. J. Stomp, Phys. Lett. 32B, 92 (1970).
[3]S. H. Fox and Sam M. Austin, Phys. Rev. C 21, 1133 (1980).
[4]W. D. Cornelius, J. M. Moss, and T. Yamaya, Phys. Rev. C 23, 1364 (1981).
[5]Y. Aoki, S. Kunori, K. Nagano, Y. Toba, and K. Yagi, Nucl. Phys. A382, 269 (1982).
[6]R. D. Bent, P. H. Pile, R. E. Pollock, and P. T. Debevec, Nucl. Instrum. Methods 180, 397 (1981).
[7]J. R. Comfort, G. L. Moake, C. C. Foster, P. Schwandt, C. D. Goodman, J. Rapaport, and W. G. Love, Phys. Rev. C 24, 1834 (1982).
[8]R. Schaeffer and J. Raynal (unpublished). Modified for relativistic kinematics and complex interactions.
[9]J. R. Comfort, Comput. Phys. Commun. 16, 35 (1978).
[10]G. Bertsch, J. Borysowicz, H. McManus, and W. G. Love, Nucl. Phys. A284, 399 (1977).
[11]Sam M. Austin, in *The (p,n) Reaction and the Nucleon-Nucleon Force,* edited by C. D. Goodman *et al.* (Plenum, New York, 1980), p. 203.
[12]W. G. Love, see Ref. 11, p. 23.
[13]W. G. Love and M. A. Franey, Phys. Rev. C 24, 1073 (1981).
[14]S. Cohen and D. Kurath, Nucl. Phys. 73, 1 (1965).
[15]N. Ensslin, W. Bertozzi, S. Kowalski, C. P. Sargent, W. Turchinetz, C. F. Williamson, S. P. Fivozinzky, J. W. Lightbody, Jr., and S. Penner, Phys. Rev. C 9, 1705 (1974).
[16]W. M. Visscher and R. A. Ferrell, Phys. Rev. 107, 781 (1957).
[17]T.-S. H. Lee and D. Kurath, Phys. Rev. C 21, 293 (1980).
[18]J. R. Comfort, Phys. Rev. C 24, 1844 (1981).
[19]D. C. Peaslee and C. F. Williamson, Phys. Rev. C 10, 1229 (1974).
[20]J. R. Comfort and B. C. Karp, Phys. Rev. C 21, 2162 (1980).
[21]M. Bister, A. Anttila, and J. Keinonen, Phys. Rev. C 16, 1303 (1977).
[22]J. W. Olness, A. R. Poletti, and E. K. Warburton, Phys. Rev. 154, 971 (1967).
[23]F. Ajzenberg-Selove, Nucl. Phys. A248, 1 (1975).
[24]J. J. Kelly, in *The Interaction Between Medium Energy Nucleons in Nuclei—1982,* Proceedings of the Workshop on the Interaction Between Medium Energy Nucleons in Nuclei, AIP Conf. Proc. No. 97, edited by H. O. Meyer (AIP, New York, 1983).
[25]J. J. Kelly, in *Spin Excitations in Nuclei,* edited by F. Petrovich (Plenum, New York, in press).